Design and Implementation of a Multi-Output Flyback Auxiliary Power Supply for Bipolar DC Grids

Yadav, Sachin; Qin, Zian; Bauer, Pavol

DOI
10.1109/PEMC61721.2024.10726350

Publication date
2024

Document Version
Final published version

Published in
2024 IEEE 21st International Power Electronics and Motion Control Conference, PEMC 2024

2024 IEEE 21st International Power Electronics and Motion Control Conference (PEMC) | 979-8-3503-8523-6/24/$31.00 ©2024 IEEE | DOI: 10.1109/PEMC61721.2024.10726350

Design and Implementation of a Multi-Output Flyback Auxiliary Power Supply for Bipolar DC Grids

1st Sachin Yadav
DC Systems, Energy Conversion & Storage
Delft University of Technology
Delft, The Netherlands
S.Yadav-1@tudelft.nl

2nd Zian Qin
DC Systems, Energy Conversion & Storage
Delft University of Technology
Delft, The Netherlands
Z.Qin-2@tudelft.nl

3rd Pavol Bauer
DC Systems, Energy Conversion & Storage
Delft University of Technology
Delft, The Netherlands
P.Bauer@tudelft.nl

***Abstract*—This article introduces an auxiliary power supply (APS) designed explicitly for bipolar DC grids, utilizing a flyback topology for robust and efficient operation. Central to our design is a high-voltage 3300 V silicon carbide (SiC) MOSFET and a planar transformer comprising one primary, one auxiliary, and two secondary windings. This APS uniquely addresses the resilience requirements of bipolar grids by enabling seamless switching between poles in the event of a pole failure, thus maintaining continuous power supply. Control is achieved through the UC3844A integrated circuit from Texas Instruments. The converter's effectiveness is demonstrated through experimental validations, confirming its suitability for advanced bipolar DC grid applications.**

***Index Terms*—DC Grids, Bipolar DC, Flyback, DC-DC Converters, Auxiliary Power Supply.**

I. Introduction

Bipolar DC (BiDC) grids present a compelling alternative to unipolar DC (UDC) grids, offering superior power handling capacity while requiring only the addition of a single conductor. Moreover, BiDC grids reduce insulation requirements for cables as only half of the voltage is applied to the cables for most of their operational duration. Full grid voltage is imposed on cable insulation only during faults, albeit for brief periods. Additionally, BiDC grids offer increased parallel paths for power flow, allowing for the energization of the grid with half the total power capacity when adequately designed. Notably, achieving this requires the neutral cable to match the cross-sectional area of the conductors for the two poles [1].

To date, research efforts have predominantly focused on power converters for creating or balancing BiDC grids, as well as on general three-port converters for source or load interface in BiDC grids [2], [3]. However, there is a conspicuous absence of research on applying auxiliary power supplies (APS) within practical BiDC grids. This absence often stems from the assumption that auxiliary power is readily available. Furthermore, much of the research on converter systems has concentrated on applications in low-voltage DC (LVDC) grids. As DC penetration increases, it is imperative to consider APS applications in medium-voltage DC grids with higher voltages. For instance, the NEN 9090 standard in the Netherlands defines voltage levels for BiDC distribution grids, including +/- 175 V, +/- 350 V, and +/- 700 V. This article focuses on designing an APS for the latter voltage level.

Thus, this paper aims to unveil the design of an APS with several key characteristics:

1) Operation at high voltages.
2) Handling of both pole-to-pole and pole-to-neutral voltages.
3) Seamless transition between pole connections or from pole-to-pole to pole-to-neutral in the event of pole failure.
4) Desirable provision of multiple isolated outputs.
5) Utilization of commercially available components with a minimal bill of materials (BOM).

Designing a converter to fulfill all these characteristics presents several challenges. Previous works, such as that proposed by Grbović et al. [4], introduced APS based on the flyback topology capable of handling higher voltages but lacking inherent compatibility with BiDC grids and exhibiting complex operation. More recently, attention has shifted towards APS for solid-state transformers (SST) operating at high voltages [5]–[7], yet these solutions fail to meet all the requirements above. Inspired by these endeavors, we propose an APS based on the flyback topology, leveraging a single MOSFET and a commercially available controller integrated circuit (IC). Furthermore, our converter features a planar

This work was supported by Nederlandse Organisatie voor Wetenschappelijk Onderzoek (NWO), grant 17628.

transformer with four windings: primary, auxiliary, and two secondary windings. Consequently, this converter's design and experimental validation are the primary contributions of this work.

The rest of the article is arranged as follows. The operation of the converter is discussed in section II. This is followed by the discussion on the design of the planar transformer for this application in section III. Two designs for the planar transformers are compared in this section. This is followed by a discussion of various aspects of the converter design, such as the MOSFET switch selection, controller IC, startup circuit, etc, in section IV. The experimental results of the converter are shown in section V. Finally, the article is concluded in section VI.

II. Converter operation

The schematic of the converter is shown in Fig. 1. The converter consists of a four-winding flyback transformer, one MOSFET, and diodes for rectification on the secondary side. The role of diodes D_{pn} and D_{nm} will be elucidated later in section IV-E.

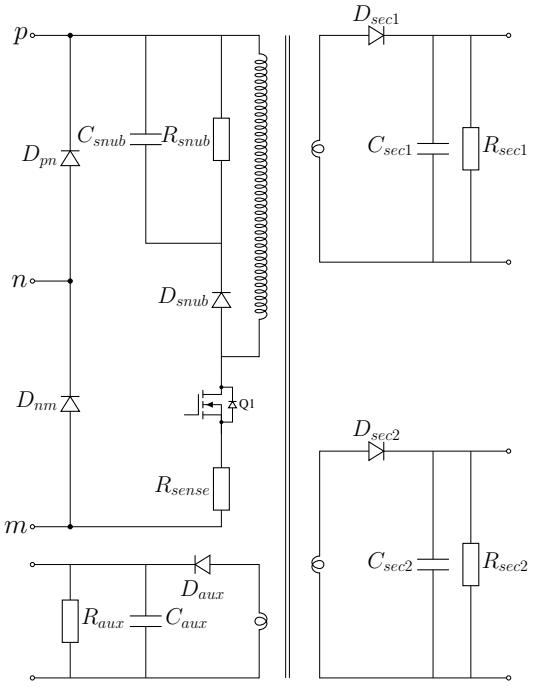

Fig. 1. Schematic of the flyback transformer.

The input parameters for the design of the converter are given in table I.

III. Planar Transformer Design

The planar transformers were designed using the scripting console in KiCad. Due to the flexibility of design in KiCad, two different designs for the transformer were tested. The printed circuit board (PCB) consisted of four standard layers. The layer stacks for the windings were different for the two designs. Each of these designs had a very different behavior. The parameters were measured using the Keysight E4990A impedance analyzer. The magnetizing inductance was measured at the primary side by keeping all the other windings open.

TABLE I
Parameters of the designed converter.

Converter parameters	Value
Min. input voltage	600 V
Max. input voltage	1500 V
Total output power	20 W
Output voltage	22 V
Number of outputs	2
Switching frequency	50 kHz

On the other hand, the leakage inductance was measured on the primary side by short-circuiting all the other windings. Before starting the converter, the designed transformers were tested for magnetizing and leakage inductance. Please note that this was done on a bare PCB without any components so that the influence of the components on the measurements can be nullified. The design considerations for the two flyback transformers and the corresponding results are discussed in detail below.

A. Design 1

In this design, the layer stack was Prim-(Sec, Aux)-Prim-(Sec, Aux). Figure 2 shows the burst-out 3D picture of the transformer. Half of the primary winding was routed on layer one and the other half on layer three. The auxiliary and two secondary windings were routed together. Like the primary winding, half of the secondary and auxiliary windings were routed on layer two and the other half on layer four. The windings on different layers were connected using vias.

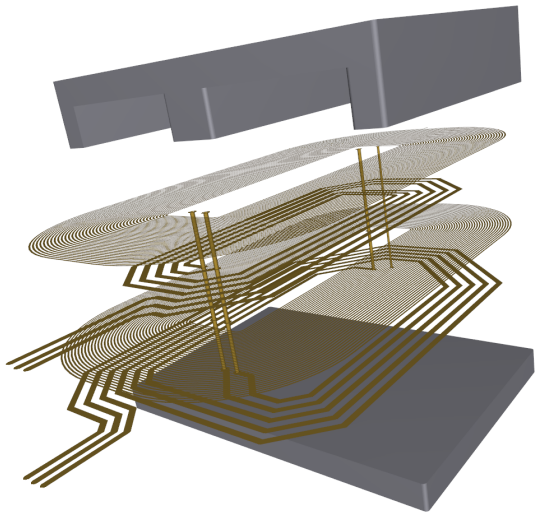

Fig. 2. Exploded 3D figure of design 1 for the planar flyback transformer.

This flyback transformer's design parameters and results are given in table II. It can be observed that the leakage inductance of this design is low. The low leakage inductance is mainly attributed to the interleaving between the primary and

other windings. On the other hand, the parasitic capacitance is relatively high. The main reason for this is speculated to be the winding structure of the primary. The capacitance is the electric field energy stored between the two conductors. In this design, it can be observed that the voltage gradient is very high at the extremities of the windings. Therefore, the stored electric field energy is high, leading to higher parasitic capacitance.

TABLE II
PARAMETERS FOR THE FIRST FLYBACK PLANAR TRANSFORMER.

Parameter	**Value**
Core shape	EILP58
Core material	3C95
Air gap	0.1 mm
Primary winding turns (N_p)	82
Auxiliary winding turns (N_{aux})	3
Secondary winding turns (N_s)	4
Results	**Value**
Magnetizing inductance	18 mH
Leakage inductance	8 µH
Parasitic capacitance	110 pF

B. Design 2

In this design, the layer stack up was (Sec, Aux)-Prim-Prim-(Sec, Aux). Figure 3 shows the 3D picture of the designed transformer. Similar to design 1, each layer had half of the corresponding windings.

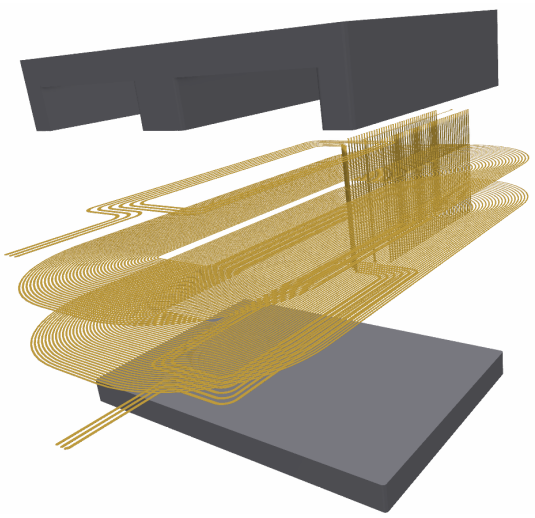

Fig. 3. Exploded 3D figure of design 2 for the planar flyback transformer.

Table III shows this flyback transformer's design parameters and results. It can be seen that contrary to design 1, the leakage inductance is higher in this design with lower parasitic capacitance. This lower parasitic capacitance can be attributed to the more spread-out electric field for the primary winding. Furthermore, the higher leakage can be attributed to the more spread-out area of the primary winding and lesser interleaving between the primary and other windings.

For this converter, a higher parasitic capacitance is undesirable. This is because a high parasitic capacitance would shift the resonant frequency of the flyback transformer closer to the switching frequency. If the resonant frequency is closer to the switching frequency, it can lead to issues in the operation as there can be significant shifts in inductance. Due to this reason, the second design of the flyback transformer is more desirable due to lower parasitic capacitance. A higher leakage inductance is not an issue, as a properly designed snubber can quickly dissipate the energy.

TABLE III
PARAMETERS FOR THE SECOND FLYBACK PLANAR TRANSFORMER.

Parameter	**Value**
Core shape	EILP58
Core material	3C95
Air gap	0.1 mm
Primary winding turns (N_p)	82
Auxiliary winding turns (N_{aux})	3
Secondary winding turns (N_s)	3
Results	**Value**
Magnetizing inductance	18 mH
Leakage inductance	24 µH
Parasitic capacitance	30 pF

IV. CONVERTER DESIGN

In this section, the selection and configuration of the various vital components of the converter are discussed.

A. Switch selection

This transformer uses a single switch, as shown in Fig. 1. The single switch was a deliberate choice to simplify the design. Furthermore, the controller IC supports only a single switch with limitations on the output gate current of 1 A.

With a single-switch design, the switch needs to handle a much higher voltage than the input voltage due to the reflected voltage from the secondary side. This voltage is given by

$$V_{sw} = V_{in} + \frac{N_p}{N_s}(V_o + V_{d,f}) \tag{1}$$

where V_{in} is the input voltage of the converter, N_p is the number of turns of the primary winding, N_s is the number of turns of the secondary winding, V_o is the output voltage at the corresponding secondary winding, and $V_{d,f}$ is the forward voltage drop of the secondary diode. Putting values from table I and III in (1), the maximum rating of the switch can be found as 2120 V. Only the 3300 V commercially available SiC MOSFETs can fulfill this voltage level. Therefore, we have selected the G2R1000MT33J MOSFET from Genesic for this converter [8].

B. Controller IC

A block diagram of the IC used in this converter is shown in Fig. 4. The main reasons for using this controller IC are as follows [9].

- Commercially available.
- Inexpensive.
- Several alternatives are available.
- Robust operation.

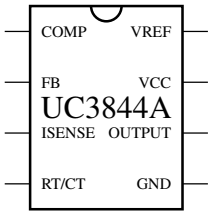

Fig. 4. IC used for this work.

- Highly customizable.

The IC is capable of controlling the flyback converter from the primary side. The IC has cycle-by-cycle limitations for the MOSFET switch's source current to ensure safe operation. Furthermore, the IC can operate at a switching frequency of up to 500 kHz. The IC has a low startup current requirement. Therefore, a high-voltage design can be created using higher values for startup and feedback resistances. All these features make this IC a suitable candidate for this work.

C. Startup circuit

Designing a correct startup circuit is very important for this IC. The converter should be able to start from the full pole-to-pole voltage and pole-to-neutral voltage. This is challenging because the startup voltage range of the converter is huge. Furthermore, selecting the correct values can be difficult due to the startup current and under-voltage lockout (UVLO) at turn-on thresholds. The startup circuit is shown in Fig. 5.

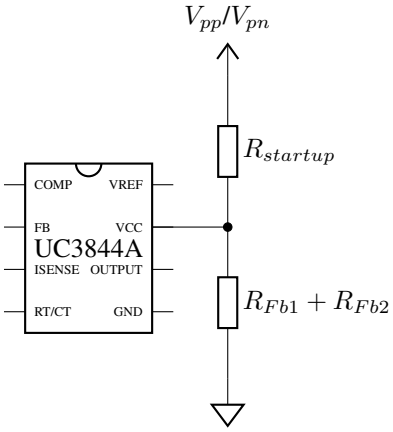

Fig. 5. Startup circuit for the flyback transformer.

There are several constraints for selecting the values of the resistances above. Firstly, the resistors should not be small enough to supply the startup current. Due to this:

$$R_{startup} \leq \frac{V_{pn}}{I_{startup}} \tag{2}$$

where $I_{startup}$ is the required current for starting the IC, and V_{pn} is the pole to neutral voltage. Here, we must consider pole to neutral voltage to find the smallest value of $R_{startup}$. Furthermore, the voltage V_{cc} should be higher than the turn-on threshold of the IC. Hence,

$$R_{startup} \leq \frac{V_{pn} - V_{cc}}{V_{cc}}(R_{Fb1} + R_{Fb2}) \tag{3}$$

Now, choosing a smaller value also presents a challenge when the IC is started from pole-to-pole voltage. When the IC is started with full voltage, the voltage V_{cc} at the IC pin should be lower than the maximum allowed value. Therefore,

$$V_{cc} = \frac{V_{pp}(R_{Fb1} + R_{Fb2})}{R_{startup} + R_{Fb1} + R_{Fb2}} \leq V_{cc,max} \tag{4}$$

where $V_{cc,max}$ is the maximum limit of the voltage for the IC. This value can be found in the datasheet.

D. Gate driver circuit

The MOSFET used in this design is a SiC MOSFET. The manufacturers of SiC MOSFETs recommend applying a negative voltage during the turn-off of the switch to minimize spurious turn-on of the switch. However, the IC used for this converter is inherently incapable of providing a negative bias. Hence, an alternative method to create a negative bias, a given in [10], is used for this converter. The schematic of the gate driver circuit is shown in Fig. 6.

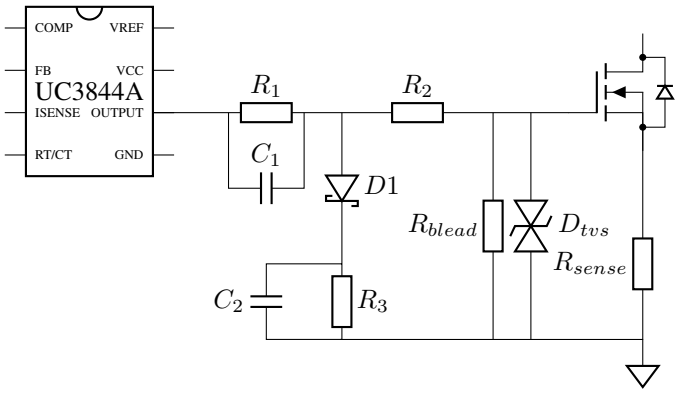

Fig. 6. Circuit used for level shifting the gate signal.

E. Pole switching

The pole-switching operation is straightforward and made possible with the help of diodes D_{pn} and D_{nm}. When one of the converters is unavailable, the diode connected in parallel takes power from the other source and supplies it to the flyback converter. This process is graphically illustrated in Fig. 7.

V. Results

Figure 8 shows the designed converter prototype. The prototype features a 3300 V MOSFET, UC3844A controller IC, and a planar transformer with four windings.

In this section, the results of the converter operation are discussed. Firstly, the important signals measured using an oscilloscope are shown in Fig. 9. The results are shown with an input voltage of 1260 V and a total output load current (sum of output 1 and 2) of 1.25 A. For clear visualization, some of the signals are scaled appropriately. This is done for the primary side switch current, representing the voltage drop

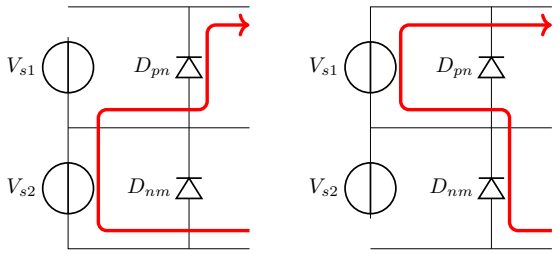

Fig. 7. Figures illustrate the current flow by a red arrow when one of the poles is out of service. Left: The converter V_{s1} is out of service; Right: The converter V_{s2} is out of service.

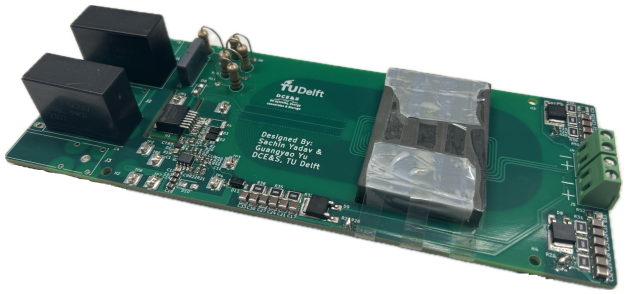

Fig. 8. Designed flyback converter.

across the resistor R_{sense}. The output has a lot of oscillations, which can be attributed to the measurement being done before the filter and impacting the sensing loop's parasitic inductance. The scaling 100:1 is also done for the drain-source voltage across the MOSFET. The gate-source voltage to the switch is represented by v_{gs}. This signal is not scaled, and it can be observed that the voltage is level-shifted using the technique discussed in section IV-D. Lastly, the output voltage (V_{out}) and auxiliary winding output (V_{dd}) are the same. This is expected, and the number of windings for the outputs and the auxiliary are the same.

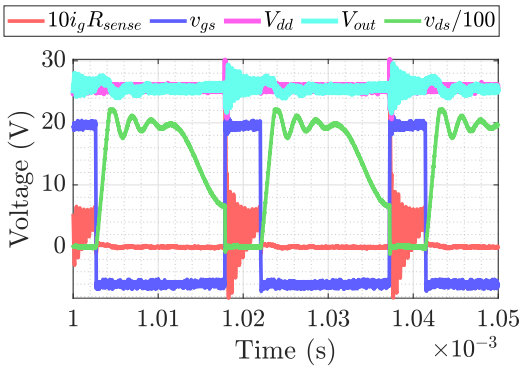

Fig. 9. Results for the converter operating at 1260 V input with 1.25 A output current.

Furthermore, the pole-switching operation results are shown below. For this test, first, the converter is turned on with full pole-to-pole voltage. With the controller turned on, the voltage at the output and the auxiliary can be observed around 25.5 V. After this, the source V_{s1} is turned off. With the load at the output same, the voltage decreases to about 21 V. After a few seconds, V_{s1} is turned on. The same procedure is repeated, but V_{s2} is turned off this time. Fig. 10 shows the resulting output and auxiliary voltages.

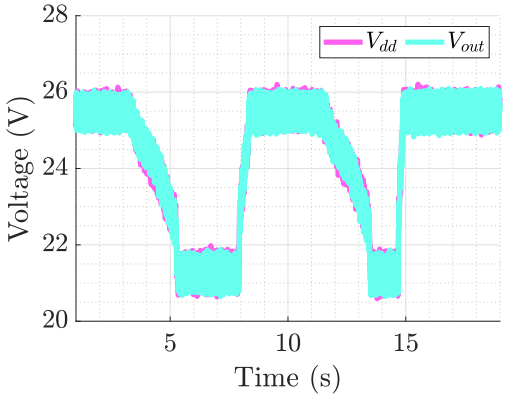

Fig. 10. Results for the pole switching operation.

VI. Conclusion

This article presents a comprehensive design and operational analysis of an auxiliary power supply (APS) tailored for bipolar DC grids, employing a flyback topology with a single MOSFET switch of 3300 V. We explored two distinct designs for the planar transformer, providing a detailed comparison to assist in selecting the optimal configuration. Furthermore, the converter utilized a commercially off-the-shelf flyback controller IC. Experimental validation confirmed the functionality of the converter in both high voltage and pole-switching operations, underpinning its potential in practical applications.

Acknowledgment

The authors thank Guangyao Yu for his input during the converter's conceptualization, design, and testing phases.

References

[1] J. Ma, M. Zhu, Y. Li, and X. Cai, "Monopolar fault reconfiguration of bipolar half bridge converter for reliable load supply in dc distribution system," *IEEE Transactions on Power Electronics*, vol. 37, no. 9, pp. 11 305–11 318, 2022.

[2] S. Rivera, R. Lizana, S. Kouro, T. Dragičević, and B. Wu, "Bipolar dc power conversion: State-of-the-art and emerging technologies," *IEEE Journal of Emerging and Selected Topics in Power Electronics*, vol. 9, no. 2, pp. 1192–1204, 2020.

[3] V. F. Pires, A. Cordeiro, C. Roncero-Clemente, S. Rivera, and T. Dragičević, "Dc-dc converters for bipolar microgrid voltage balancing: A comprehensive review of architectures and topologies," *IEEE Journal of Emerging and Selected Topics in Power Electronics*, 2022.

[4] P. J. Grbovic, "High-voltage auxiliary power supply using series-connected mosfets and floating self-driving technique," *IEEE Transactions on Industrial Electronics*, vol. 56, no. 5, pp. 1446–1455, 2009.

[5] S. Zong, Q. Zhu, W. Yu, and A. Q. Huang, "Auxiliary power supply for solid state transformer with ultra high voltage capacitive driving," in *2015 IEEE Applied Power Electronics Conference and Exposition (APEC)*. IEEE, 2015, pp. 1008–1013.

[6] J. Liu, S. Zhong, J. Zhang, Y. Ai, N. Zhao, and J. Yang, "Auxiliary power supply for medium-/high-voltage and high-power solid-state transformers," *IEEE Transactions on Power Electronics*, vol. 35, no. 5, pp. 4791–4803, 2019.

[7] S. Ren, C. Li, L. Zhu, W. Li, X. He, and W. Qu, "Analysis and modeling of self-powered cascaded resonant switched capacitor power supply for medium voltage dc systems," *IEEE Transactions on Power Electronics*, 2023.
[8] *G2R1000MT33J 3300 V 1000 mOhm SiC MOSFET*, GeneSic Semiconductors, 8 2020, rev. 1.
[9] *UCx84xA Current-Mode PWM Controller*, Texas Instruments Incorporated, 7 2022, rev. G.
[10] J. Wang and H. S.-H. Chung, "A novel rcd level shifter for elimination of spurious turn-on in the bridge-leg configuration," *IEEE Transactions on Power Electronics*, vol. 30, no. 2, pp. 976–984, 2014.